Oxygen blocks the reaction of the FixL−FixJ complex with ATP but does not influence binding of FixJ or ATP to FixL

ARTICLE *in* BIOCHEMISTRY · DECEMBER 2005

Impact Factor: 3.02 · DOI: 10.1021/bi051661h · Source: PubMed

Oxygen Blocks the Reaction of the FixL−FixJ Complex with ATP but Does Not Influence Binding of FixJ or ATP to FixL†

Eduardo Henrique Silva Sousa, Gonzalo Gonzalez, and Marie-Alda Gilles-Gonzalez*

Department of Biochemistry, University of Texas Southwestern Medical Center, 5323 Harry Hines Boulevard, Dallas, Texas 75390-9038

Received August 19, 2005; Revised Manuscript Received September 23, 2005

ABSTRACT: The *Rm*FixL−*Rm*FixJ oxygen signal transduction system ensures that a cascade of the *Sinorhizobium meliloti* nitrogen fixation genes is induced as the concentration of O_2 drops below 50 μM in symbiotic nodules. Deoxy-*Rm*FixL is a histidine protein kinase that catalyzes a phosphoryl transfer from ATP to the aspartate 54 residue of *Rm*FixJ; *Rm*FixJ is a response regulator that becomes activated as a transcription factor by phosphorylation. Association of O_2 with a heme-binding domain in *Rm*FixL triggers a conformational change that inhibits its kinase activity. Here we consider whether this inhibition is achieved by disrupting binding of either of the substrates, i.e., *Rm*FixJ or ATP, to the *Rm*FixL kinase. The ATP affinities of the oxy and deoxy states were compared via competition of ATP against TNP-nucleotide fluorophores. The influence of O_2 on formation of the *Rm*FixL−*Rm*FixJ complex was investigated by fluorescence polarization. Oxygen dramatically inhibited the reaction of the *Rm*FixL−*Rm*FixJ complex with ATP but affected neither ATP binding ($K_d \sim 100$ μM) nor *Rm*FixL−*Rm*FixJ complex formation ($K_d \sim 4$ μM), indicating that inhibition of the kinase by the oxy-heme in *Rm*FixL is achieved by inactivating the catalytic site, rather than by blocking the association of this enzyme with either of its substrates. An 8-fold enhancement of the rate of reaction of *Rm*FixL with ATP in a deoxy-*Rm*FixL−D54N *Rm*FixJ complex, compared to that in isolated deoxy-*Rm*FixL, exposes the strength of the allosteric effect of *Rm*FixJ on the reaction. These results clarify the mechanistic roles of the signal and regulatory partner in this signal transduction system.

The *Rm*FixL−*Rm*FixJ[1] O_2 signal transduction system responds to a drop in physiological O_2 concentration by triggering a cascade of new gene expression (*1*). The changed expression leads to the production of alternative high-O_2 affinity oxidase for microaerobic respiration and, in many nitrogen-fixing bacteria, the nitrogenase enzymes and their accessory proteins (*1*−*8*). The *Rm*FixL and *Rm*FixJ proteins are essential for the symbiotic association of the nitrogen-fixing bacterium *Sinorhizobium meliloti* with alfafa root nodules and production of more than 20 new proteins for the nitrogen fixation process (*1*, *4*).

*Rm*FixL and *Rm*FixJ belong to the family of two-component regulatory systems that are ubiquitous in microorganisms (*9*−*13*). Such modular systems play vital roles in stimulus−response coupling and adaptation to environmental changes. They typically employ a sensor protein and a response regulator protein, with input and output modules, respectively, that are specific to their sensing functions. At the same time, they feature a conserved enzymatic module in the sensor and a conserved regulatory module in the response regulator that permit a preserved phosphoryl-transfer mechanism (*10*, *11*). The FixL−FixJ system holds a special place among the two-component regulatory systems because of its great simplicity and well-characterized signal-detection element. Specifically, reversible binding of O_2 to a heme moiety in *Rm*FixL is known to couple to a kinase activity (*14*−*16*). Normoxic conditions inhibit the kinase (*15*, *16*). Hypoxic conditions trigger transduction of the signal by a phosphoryl transfer to the transcription factor *Rm*FixJ (*15*−*18*). For the majority of two-component systems, a clear picture of how signal is sensed and coupled to the kinase remains one of the outstanding challenges. The FixL−FixJ system offers the advantage of putting the full signal response under kinetic investigation.

All FixL proteins contain three identifiable regions: a variable N-terminal domain, a central heme-binding domain, and a C-terminal histidine protein kinase region (*19*). Likewise, all FixJ proteins have at least two regions: a phosphorylatable N-terminal receiver domain and a C-terminal DNA-binding domain (*10*, *18*). In FixL, the heme-binding and kinase regions are necessary and sufficient for a regulated response to O_2 (*14*, *15*). The version of *Rm*FixL traditionally studied is *Rm*FixLT, a soluble form, from which a hydrophobic N-terminal region is excised (*14*). In the

†This project was supported by the National Research Initiative of the USDA Cooperative State Research, Education and Extension Service Grant Number 2002-35318-14039 and by Welch Foundation Grant I-1575.

* To whom correspondence should be addressed. Telephone: (214) 648-9438. Fax: (214) 648-8856. E-mail: magg@biochem.swmed.edu.

[1] Abbreviations: *Rm*FixL, *S. meliloti* (formerly *Rhizobium meliloti*) FixL; *Rm*FixLT, soluble *Rm*FixL containing the heme-binding domain followed by a histidine kinase domain (in this work, *Rm*FixLT and *Rm*FixL are used interchangeably); *Rm*FixJ, *S. meliloti* FixJ; *Rm*FixLJ, complex of *Rm*FixL with *Rm*FixJ; deoxy, Fe^{II} without ligand; oxy, $Fe^{II}O_2$; met, Fe^{III} without ligand; cyanomet, $Fe^{III}CN^-$; TNP-ATP, 2′-(3′)-*O*-(2,4,6-trinitrophenyl)adenosine 5′-triphosphate; TNP-ADP, 2′-(3′)-*O*-(2,4,6-trinitrophenyl)adenosine 5′-diphosphate.

10.1021/bi051661h CCC: $30.25
Published on Web 10/29/2005

*Rm*FixL−*Rm*FixJ system, saturation of the heme with O_2 inhibits the kinase activity more than 100-fold, whereas removal of O_2 restores full activity (*16*, *20*). The deoxy form of *Rm*FixL catalyzes transfer of a γ-phosphoryl group from ATP to a conserved aspartate residue (Asp 54) in *Rm*FixJ, with an intermediate phosphorylation of a conserved histidine residue (His 285) in *Rm*FixL (*15*, *21*, *22*). Phosphorylation of *Rm*FixJ triggers a conformational change that enhances the dimerization of this transcription factor and its affinity for target sites in DNA (*17*, *18*, *23*). The *Rm*FixL kinase region encompassing His 285 and the *Rm*FixJ receiver domain containing Asp 54 are conserved throughout the family of two-component regulatory systems (*10*, *11*).

A recently proposed revised scheme assumes that the formation of a complex of *Rm*FixL with both *Rm*FixJ and ATP precedes all phosphoryl transfers (*16*, *24*). This revision was prompted by the following observations. The inclusion of *Rm*FixJ alters the initial response to heme ligands and, most notably, increases the specificity of the response to O_2 (*16*). *Rm*FixJ causes a 10-fold acceleration of the phosphorylation of *Rm*FixL and a 4-fold increase in the equilibrium levels of phospho-*Rm*FixL (*24*). When the phosphoryl transfers from ATP to *Rm*FixL and from phospho-*RmFixL* to *Rm*FixJ are carried out sequentially, the rates of these reactions are so slow (0.019 and 0.116 min^{-1}, respectively) and the loss of phosphate from phospho-*Rm*FixJ is so rapid that accumulation of phospho-*Rm*FixJ for regulation is rendered impossible (*15*). There are at least five steps that O_2 could regulate.

complex formation

$$\textit{Rm}\text{FixL}_2 + \textit{Rm}\text{FixJ}_2 \rightleftarrows \textit{Rm}\text{FixL}_2\cdot\textit{Rm}\text{FixJ}_2$$

nucleotide binding

$$\textit{Rm}\text{FixL}_2\cdot\textit{Rm}\text{FixJ}_2 + 2\text{ATP} \rightleftarrows \textit{Rm}\text{FixL}_2\cdot\textit{Rm}\text{FixJ}_2\cdot 2\text{ATP}$$

*Rm*FixL phosphorylation

$$\textit{Rm}\text{FixL}_2\cdot\textit{Rm}\text{FixJ}_2\cdot 2\text{ATP} \rightleftarrows (\text{P-}\textit{Rm}\text{FixL}\cdot\textit{Rm}\text{FixJ})_2 + 2\text{ADP}$$

phosphoryl transfer

$$(\text{P-}\textit{Rm}\text{FixL}\cdot\textit{Rm}\text{FixJ})_2 \rightleftarrows (\textit{Rm}\text{FixL}\cdot\textit{Rm}\text{FixJ-P})_2$$

*Rm*FixJ dissociation

$$(\textit{Rm}\text{FixL}\cdot\textit{Rm}\text{FixJ-P})_2 \rightleftarrows \textit{Rm}\text{FixL}_2 + \text{P-}\textit{Rm}\text{FixJ}_2$$

We set out to elucidate the effect of O_2 on the first four of these mechanistic steps. Our strategy for examining whether binding of ATP is a potential site for O_2 regulation exploits the fluorescence of TNP-nucleotide probes. Nucleotide binding sites in a number of proteins, including two-component systems, have been investigated with these fluorophores (*25*−*27*). They typically show good fluorescence enhancement on binding to proteins, a high Stokes shift, and an unusually high affinity for nucleotide binding sites (*26*). For investigating the influence of O_2 on complex formation, we turned to fluorescence polarization. Finally, we look at the combined roles of O_2 and *Rm*FixJ allostery in the reaction with ATP by examining the consequence of having a partner *Rm*FixJ that cannot be phosphorylated. The system thus freed of concurrent phosphoryl transfers allows a clearer view of this phosphorylation.

EXPERIMENTAL PROCEDURES

Gene Expression and Protein Purifications. The *S. meliloti* *Rm*FixLT protein, consisting of heme-binding and kinase domains, was derived from a gene overexpressed in *Escherichia coli*. The procedures for overexpression and purification were previously described (*28*). The T2C *Rm*FixJ and D54N *Rm*FixJ variants were prepared by site-directed mutagenesis of the *RmfixJ* gene cloned in a plasmid (QuickChange protocol, Stratagene). All final constructs contained the gene segment under *tac*-promoter control on plasmids conferring ampicillin resistance. Mutations were confirmed by sequencing both strands of each DNA segment. The plasmids were transformed into *E. coli* strain TG1 and overexpressed and purified as previously described (*15*, *28*).

Fluorophore Labeling of Proteins. The T2C *Rm*FixJ variant was labeled at the cysteine introduced near its N-terminus, with a Texas Red C_2-maleimide probe (Molecular Probes, Inc.). Briefly, the protein solution was rid of β-mercaptoethanol by being passed through a gel filtration column and maintained in an excess of tris(2-carboxyethyl)-phosphine hydrochloride (TCEP). The fluorescent label was added to protein inside an anaerobic glovebag (Coy Laboratories, Inc.), and the reaction was stopped with 5 mM dithiothreitol (DTT). The excess of free Texas Red was removed by gel filtration. The labeled protein was quantified with the Bradford assay (Bio-Rad dye reagent concentrate) using bovine serum albumin as the standard (*29*). The efficiency of labeling was 96%, as determined by assuming a Texas Red absorbtivity of 112 mM^{-1} cm^{-1} at the absorption maximum of 590 nm.

Steady-State Fluorescence of Bound Nucleotides. Measurements were carried out on a Fluoromax-3 spectrofluorimeter (Jobin Yvon-Horiba, Inc., Edison, NJ) in quartz fluorescence microcuvettes with a path length of 5 mm (Starna Cells, Inc.) at 25 °C. For most of the experiments, the excitation and emission slit apertures were 4 nm. Precautions were taken to minimize and correct for inner filter effects, and alternative excitation wavelengths were selected whenever appropriate. For example, to minimize the influence of the Soret peak, the excitation was set at 470 nm for the TNP-labeled nucleotides.

Binding of TNP-ATP to protein was assessed by the fluorescence intensity change at 540 nm after subtraction of a blank containing all the reaction components except the protein. The samples were kept in phosphorylation buffer [50 mM Tris (pH 8.0), 50 mM KCl, 5.0% ethylene glycol, and 0.50 mM $MgCl_2$]. The TNP-nucleotide concentrations were determined spectrophotometrically, assuming an absorbtivity of 26 mM^{-1} cm^{-1} at 408 nm (*30*). For some experiments, the magnesium was replaced with manganese or the divalent cation was omitted, as noted. The titrations of *Rm*FixL with TNP-ATP or TNP-ADP were conducted by adding microliter quantities (40−1600 pmol) of these probes into a microcuvette with 0.40 mL of *Rm*FixL (2−4 μM) in either the met or cyanomet form (2.0 mM KCN included), and with or without a 10-fold excess of *Rm*FixJ. For all these titrations, the heme state was checked by UV−vis spectroscopy before, during, and after the experiments

(Cary 4000 UV−vis spectrophotometer, Varian). The samples were mixed with the TNP-labeled nucleotide for 1 min before acquisition of data, and three readings were averaged. The fluorescence intensities were corrected for dilution whenever the dilution exceeded 5% of the original volume.

Competition Titrations for Ferric Forms. The initial solutions contained 4 μM met- or cyanomet-*Rm*FixL in phosphorylation buffer, with or without a 10-fold excess of *Rm*FixJ, and with 12 μM TNP-ADP. Concentrated ATP was added to this mixture in microliter quantities (20−1800 nmol), and the decrease in fluorescence was monitored. The fluorescence of a control sample containing 12 μM TNP-ATP and high concentrations of ATP ($\sim$3 mM), but no protein, was taken as a reference for the fully displaced probe.

Competition Titrations for Ferrous Forms. The competition mixtures (400 μL) contained 4 μM oxy- or deoxy-*Rm*FixL in phosphorylation buffer, 40 μM *Rm*FixJ, and 6 μM TNP-ADP. This buffer was supplemented with 10 mM ascorbic acid and a mixture of glucose oxidase and catalase (99:1, 3.5 μL, Sigma Chemicals, Inc.) and glucose (4 mM), as noted. Each set of experiments assayed the competition by ATP at three ATP concentrations: 0.285, 1.0, and 2.5 mM. Initially, the fluorescence emission was measured for the oxy-*Rm*FixL/*Rm*FixJ mixture containing TNP-ATP along with the competitor ATP and the glucose oxidase/catalase mixture. Removal of O_2 was initiated by adding glucose (4 mM) and immediately sealing this reaction mixture. The progress of the reaction and production of deoxy-*Rm*FixL were followed from the fluorescence signal and UV−vis absorption, respectively, measured over 20 min. The fluorescence intensity for aerobic samples was taken as the 100% point and compared to the values obtained for the corresponding anaerobic samples. A control reaction to verify the rate of the conversion from oxy-*Rm*FixL to deoxy-*Rm*FixL was also run under conditions similar to those of the experiment described above.

Data Analysis. The fluorescence data were treated as previously described by Kenney, Adams, and their colleagues (*25*, *31*). The observed changes in fluorescence at any given concentration of TNP derivative (ΔF) were normalized to the total change in fluorescence at infinite concentration (ΔF_{max}) to obtain the ratio $\Delta F/\Delta F_{max}$. Titration data were fit to the following quadratic equation:

$$\frac{\Delta F}{\Delta F_{max}} = \frac{K_d + L_t + E_t - \sqrt{(K_d + L_t + E_t)^2 - 4L_tE_t}}{2E_t} \quad (1)$$

where L_t and E_t are the local concentrations of ligand and protein, respectively, and K_d is the dissociation constant. The true K_d values for the competing ligands were calculated according to eq 2:

$$^{App}K_d^{ATP} = K_d^{ATP}\left(1 + \frac{L}{K_d^{L}}\right) \quad (2)$$

where L is the concentration of the competing fluorophore (TNP-ADP) and K_d^{ATP} and K_d^{L} are the equilibrium dissociation constants for binding of ATP and TNP-ADP, respectively.

Fluorescence Polarization Measurements of Formation of the RmFixLJ Complex. Texas Red-labeled T2C *Rm*FixJ (0.5 μM) was titrated with ferrous *Rm*FixL in phosphorylation buffer under anaerobic or aerobic conditions at 25 °C. To ensure the absence of O_2 during the anaerobic titrations, the labeled T2C *Rm*FixJ was maintained in 5 mM DTT and a mixture of glucose and glucose oxidase with catalase (99:1). The deoxy-*Rm*FixL was prepared in an anaerobic glovebag; an excess of DTT was added, and it was kept in a septum-sealed microcentrifuge tube, on ice, until withdrawal of small aliquots with a gastight syringe. The state of the *Rm*FixL in the *Rm*FixL/*Rm*FixJ−Texas Red mixture in the fluorescence cuvette was verified as being fully deoxy by UV−vis spectroscopy. For aerobic experiments, the proteins were kept in 10 mM 2-mercaptoethanol in an open cuvette, with frequent aeration. UV−vis spectra were recorded to verify full conversion to the oxy form without oxidation. Before each set of experiments, the polarizer alignment was checked with a Ludox suspension. The excitation and emission slits were set to 5 nm. Two excitation wavelengths, 550 and 590 nm, were selected to minimize the influence of the α/β heme peaks. After each addition of *Rm*FixL to the labeled *Rm*FixJ, the protein mixture was equilibrated for $\sim$1 min, and the fluorescence polarization was measured twice, at intervals of $\sim$ 20 s. A typical binding experiment lasted $\sim$30 min.

Phosphorylation Assays. The reactions of *Rm*FixL with T2C *Rm*FixJ, D54N *Rm*FixJ, and wild-type *Rm*FixJ were performed essentially as previously described for *Rm*FixL and *Rm*FixJ (*16*). Briefly, *Rm*FixL (0.5 μM) was incubated with one of the *Rm*FixJ proteins (12.5 μM) in phosphorylation buffer [50 mM Tris (pH 8.0), 50 mM KCl, 5.0% ethylene glycol, and 0.50 mM $MgCl_2$]. For all the reactions, the oxidation state and liganded state of the *Rm*FixL were verified from the 250−700 nm absorption spectra. Reactions were begun by introducing 1 mM [γ-^{32}P]ATP (unlabeled ATP from Roche and γ-^{32}P-labeled ATP from Amersham Biosciences) at 23 °C. The reactions were stopped by mixing aliquots (20 μL) of the reaction mixtures with $^1/_3$ volume of "stop buffer" [4.0 mM EDTA, 4.0% (w/v) sodium dodecyl sulfate, 0.50 M Tris-HCl, 0.20 M NaCl, 50% (v/v) glycerol, and 2.0% (v/v) β-mercaptoethanol (pH 6.8)]. The products were electrophoresed on 15% (w/v) polyacrylamide gels (*32*). The phosphorylated protein in the dried gels was quantified with a phosphorimager (Bio-Rad Personal Molecular Imager FX).

RESULTS

Binding of TNP-Labeled Nucleotides to RmFixL. The heme group had a sufficiently low quenching effect on the fluorescence of the TNP-nucleotide probes on binding to *Rm*FixL compared to non-heme-binding histidine protein kinases, such as EnvZ and CheA, to allow affinity measurements (*25*, *27*). In particular, binding of TNP-labeled nucleotides to *Rm*FixL enhanced the nucleotide fluorescence $\sim$3-fold for *Rm*FixL concentrations of >2 μM (Figure 1A). For binding of TNP-ADP to *Rm*FixL, at pH 8.0 and 25 °C, the equilibrium dissociation constant was 1.1 $\pm$ 0.1 μM (Figure 1B and Table 1). The equilibrium dissociation constant for binding of TNP-ATP was slightly lower, 0.8 $\pm$ 0.2 μM (Table 1). The same value was measured for the met and cyanomet forms, either alone or with *Rm*FixJ, and for protein with added Mg^{2+} or Mn^{2+}. A similar metal insensitivity of TNP nucleotide binding has been observed

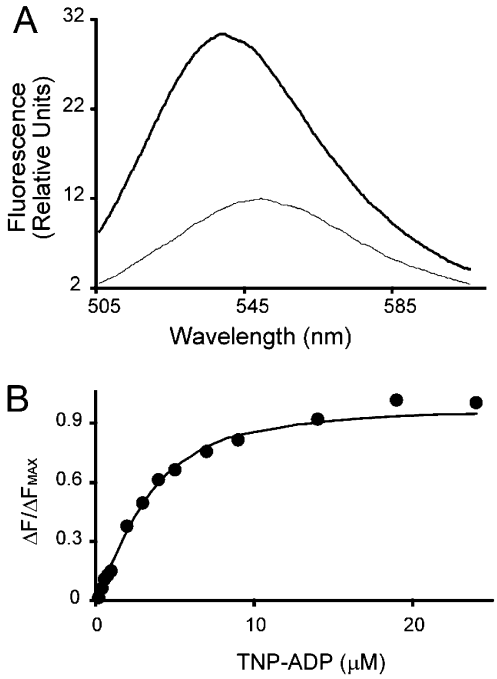

FIGURE 1: Equilibrium binding of TNP-labeled nucleotides to *Rm*FixLT at pH 8.0 and 25 °C. Panel A compares the fluorescence spectra of TNP-ATP (12 μM) alone (thin line) and in the presence of *Rm*FixLT (4 μM) (thick line), with excitation at 470 nm. Panel B shows a titration of met-*Rm*FixL (4 μM) with TNP-ADP, measured by the fluorescence intensity changes (ΔF) at 540 nm.

Table 1: Equilibrium Dissociation Constants for *Rm*FixL at 25 °C with Buffer (pH 8.0)

	K_d (μM)		K_d (μM)
TNP-ATP	0.8	TNP-ADP/*Rm*FixJ	1.1
TNP-ATP/*Rm*FixJ	0.8	ATP	104
TNP-ADP	1.1	*Rm*FixJ	4.0

for the EnvZ protein (*25*). These relatively high affinities and their insensitivity to divalent metals suggest that some of the residues for docking of the TNP-nucleotides to the ATP binding site differ from the ones for the natural nucleotides. This observation has been reported for related two-component systems, and the X-ray crystallographic structure of the CheA protein bound to TNP-ATP shows this feature (*33*). Nevertheless, a large excess of ATP fully displaces these probes from the nucleotide-binding sites, as happens in *Rm*FixL, indicating that they bind specifically to those sites (Figure 2A).

Influence of Heme Status on ATP Binding. We evaluated the effect of heme status on ATP binding by measuring the affinity of ATP for various *Rm*FixL species based on the displacement of TNP-ADP by ATP. For the ferric forms, there was no significant difference in the affinity of ATP for met- or cyanomet-*Rm*FixL in a 10-fold excess of *Rm*FixJ (Figure 2A). The measured K_d value of 104 $\pm$ 10 μM agreed closely with the previously measured K_m for ATP (Table 1) (*16*). Analogous experiments with the related *Bradyrhizobium japonicum* system, i.e., *Bj*FixL−*Bj*FixJ, also showed no effect of the heme status on the affinity for ATP (data not shown).

For the ferrous forms, we examined the identical reaction mixture with and without O_2 by introducing an O_2-scrubbing glucose/glucose oxidase/catalase system into an aerobic

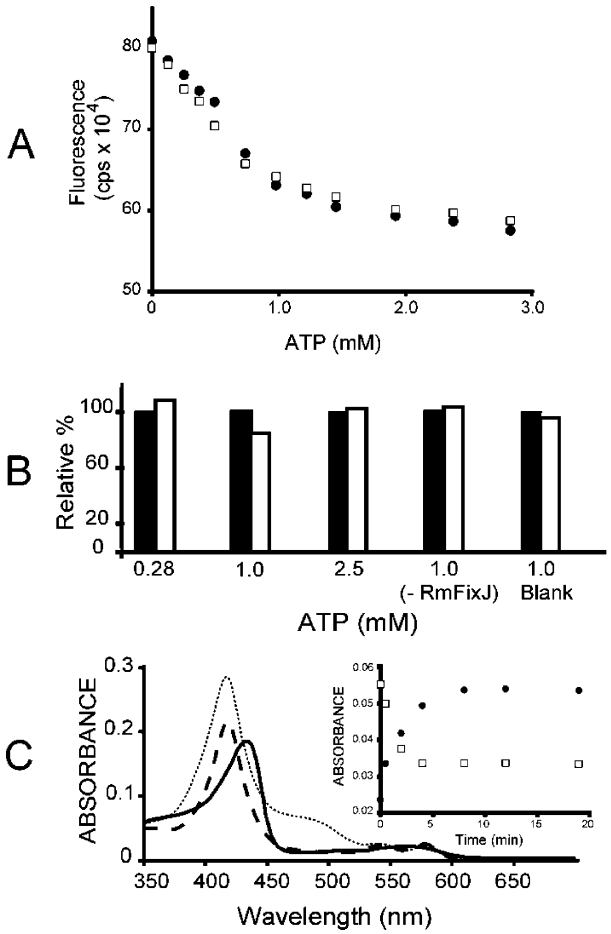

FIGURE 2: Effect of ligands on ATP affinity at pH 8.0 and 25 °C. Panel A shows the displacement of TNP-ADP (12 μM) by ATP from the met (●) and cyanomet (□) forms of *Rm*FixLJ (4 and 40 μM, respectively). All binding reaction mixtures contained 0.5 mM $MgCl_2$. The fluorescence of TNP-ADP in the absence of *Rm*FixLJ was 56 $\times$ 10^4 cps. Panel B shows the effect of O_2 on ATP affinity by competition of this nucleotide against TNP-ADP bound to *Rm*FixLJ (4 and 40 μM) in the oxy (black bars) or deoxy form (white bars); the total estimated error is $\pm$7%. The error in the ATP concentration due to active *Rm*FixL was less than 0.6%. Relative % was calculated by dividing the fluorescence intensities for the anaerobic samples by the values obtained for the corresponding aerobic samples. A control reaction to verify the time required for complete conversion of oxy- to deoxy-*Rm*FixL was also conducted under the same conditions. Oxygen saturation of FixL was the same at all ATP concentrations. Panel C shows the electronic spectrum of oxy-*Rm*FixLJ in a mixture of TNP-ADP and 1 mM ATP (···), the same sample with the TNP-ADP spectrum subtracted (− − −), and the same sample in the deoxy form with the spectrum of TNP-ADP subtracted (−). The inset shows the UV−vis monitoring of the conversion of oxy-*Rm*FixLJ to the deoxy form with the glucose/glucose oxidase/catalase system at the 430 nm deoxy peak (●) and 417 nm oxy peak (□). The initial oxygen saturation of *Rm*FixL in the air-saturated ATP solution was 92%, the same as that for *Rm*FixL in the solution free of ATP.

mixture and sealing the reaction mixture to generate the deoxy form (Experimental Procedures). To ensure that the oxy-*Rm*FixL was being converted quickly and fully to deoxy-*Rm*FixL, we monitored this conversion by UV−vis spectroscopy. Within 10 min, the oxy species was fully converted to the deoxy form under the same conditions that were used for the fluorescence measurements (inset of Figure 2C). The influence of O_2 on ATP affinity was measured for binding of three concentrations of ATP (0.285, 1.0, and 2.5 mM) to oxy-*Rm*FixL in the presence of *Rm*FixJ (1:10 FixL:FixJ ratio)

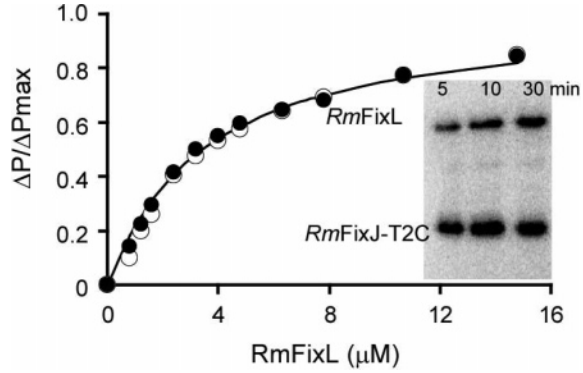

FIGURE 3: Effect of O_2 on *Rm*FixLJ complex formation at pH 8.0 and 25 °C. Binding of *Rm*FixL to Texas Red-labeled T2C *Rm*FixJ (0.5 μM), as monitored by fluorescence polarization changes (ΔP) under aerobic (●) and anaerobic (○) conditions, with 0.5 mM $MgCl_2$. The inset shows an autoradiogram of the *Rm*FixL (0.5 μM) phosphorylation of T2C *Rm*FixJ (12.5 μM) with ATP (1.0 mM).

and TNP-ADP (6 μM). The fluorescence intensity of oxy-*Rm*FixLJ was taken to be 100%, and the fluorescence intensity was followed over 20 min after addition of glucose. The switch from oxy to deoxy did not alter the relative fluorescence signal, indicating that O_2 does not significantly influence ATP affinity (Figure 2B). Similar experiments on *Rm*FixL without *Rm*FixJ also showed no effect of O_2 on ATP binding (Figure 2B).

Effect of O_2 on RmFixLJ Complex Formation. We have hypothesized that O_2 might regulate *Rm*FixLJ complex formation. In such a case, under aerobic conditions, the two proteins would have little affinity for each other, but under anaerobic conditions, their affinity for each other would sharply increase, enhancing complex formation. We exploited fluorescence polarization to address this question and selected as our fluorophore the Texas Red label employing maleimide for the coupling chemistry. *Rm*FixJ offers multiple advantages for these experiments. First, it naturally lacks a cysteine residue, and therefore, one can be introduced at a specific site in the protein for labeling by maleimide. Second, the relatively low monomeric molecular mass of *Rm*FixJ (22 kDa) should cause its labeling to result in a greater polarization change on complex formation than *Rm*FixL labeling. In particular, upon complex formation, the *Rm*FixJ switches from being monomeric to becoming part of a 133 kDa *Rm*$FixL_2$·*Rm*$FixJ_2$ complex. On the basis of the X-ray crystallographic structures of phosphorylated and unphosphorylated *Rm*FixJ, the N-terminal end of the protein appeared sufficiently far from the phosphorylation site and dimerization surfaces to tolerate residue substitutions without any damage to the protein's functions (*34*).

We prepared a T2C *Rm*FixJ variant and verified that this protein could be phosphorylated. As shown in the inset of Figure 3, the T2C *Rm*FixJ variant remained fully active. This protein was labeled with Texas Red at ~96% efficiency (Experimental Procedures). For anaerobic experiments, the Texas Red-labeled T2C *Rm*FixJ (0.5 μM) was titrated with deoxy-*Rm*FixL in an anaerobic septum-sealed cuvette, and formation of the *Rm*FixLJ complex was assessed by fluorescence polarization. Consistent with complex formation, after each *Rm*FixL addition there was a significant increase in the extent of polarization corresponding to a K_d value of 4.0 ± 0.3 μM for binding of *Rm*FixL to *Rm*FixJ at pH 8.0 and 25 °C (Figure 3). This directly measured binding constant agreed with the previously determined K_m for RmFixJ (*16*). The lack of an O_2 effect excludes *Rm*FixLJ complexation as a ligand-regulated step in the phosphoryl-transfer reactions.

The relatively low affinity of *Rm*FixL for *Rm*FixJ falls within the range observed for related prokaryotic two-component regulatory systems such as CheA−CheY (K_d ~ 2 μM) and EnvZ−OmpR (K_d ~ 0.4 μM) (*35*−*37*). For these proteins, these values represent more than 85% complexation in vivo (*38*−*40*). Such estimates of in vivo complexation are much more complex for *S. meliloti*, because it is relatively difficult to isolate symbiotic bacteroids and preserve them in an unchanged state for protein determinations. Bacteroids are a highly differentiated state of *S. meliloti* that completely fill plant nodule cells. They do not divide (there is no room for them to do so), yet they are unlike stationary cultures in that all of their metabolic needs are satisfied by the host legume. The protein profile in bacteriods is quite different from that of any free-living state of *S. meliloti*. In vegetative *S. meliloti*, the *Rm*FixL−*Rm*FixJ concentration is ~0.2 μM (M.-A. Gilles-Gonzalez, unpublished results), but in the nondividing bacteroids, these proteins might well accumulate to the micromolar levels sufficient for signaling by this system.

Influence of O_2 on the Reaction of the RmFixL−RmFixJ Complex with ATP. In *Rm*FixJ, the main phosphoryl acceptor is the Asp 54 residue, as predicted from its homology to CheY, VirG, and NtrC, and supported by the impaired phosphorylation of *Rm*FixJ proteins with substitutions of this residue (*1*, *22*). The D54N *Rm*FixJ variant represents a valuable tool for quantifying the effects of O_2 on the phosphorylation of *Rm*FixL in the *Rm*FixLJ complex. Moreover, phosphorylations of the *Rm*FixL−D54N *Rm*FixJ complex can serve to highlight the enhancement of *Rm*FixL autophosphorylation brought on by *Rm*FixJ, without the complications of additional phosphoryl transfers pulling the phosphoryl groups from *Rm*FixL to *Rm*FixJ. The initial rate of the anaerobic phosphorylation of *Rm*FixL in the *Rm*FixL−D54N *Rm*FixJ complex (1:25) was 8-fold faster than that of isolated *Rm*FixL (Figure 4). In contrast, the steady-state levels of phosphorylated *Rm*FixL in the *Rm*FixL−*Rm*FixJ (1:25) complex were nearly undetectable under turnover conditions (Figure 4). The residual D54N *Rm*FixJ phosphorylation persisting despite of the loss of the main acceptor residue is due to a much less efficient phosphoryl transfer to other acidic residues in the phospho-acceptor pocket (*22*). Since neither isolated *Rm*FixL nor the *Rm*FixL−D54N *Rm*FixJ complex can efficiently proceed with phosphoryl transfers through the complex, this enhancement of *Rm*FixL phosphorylation fully exposes a strong allosteric effect of *Rm*FixJ on the initial phosphorylation of *Rm*FixL with ATP.

We evaluated the effect of O_2 on the phosphorylation of *Rm*FixL under "turnover" conditions, employing a 25-fold excess of D54N *Rm*FixJ. As shown in Figure 4, atmospheric O_2 strongly inhibits the reaction with ATP. The finding that the inhibition due to O_2, i.e., a 13-fold inhibition factor, is essentially the same for the *Rm*FixL−D54N *Rm*FixJ complex and for the *Rm*FixL−*Rm*FixJ complex argues that O_2 does not regulate phosphoryl transfer to *Rm*FixJ (*16*). When corrected for the relatively low affinity of *Rm*FixL for O_2 (K_d ~ 50 μM), this inhibition is effectively total. When phospho-*Rm*FixL is prepared without *Rm*FixJ under anaerobic conditions and later combined with *Rm*FixJ, the phos-

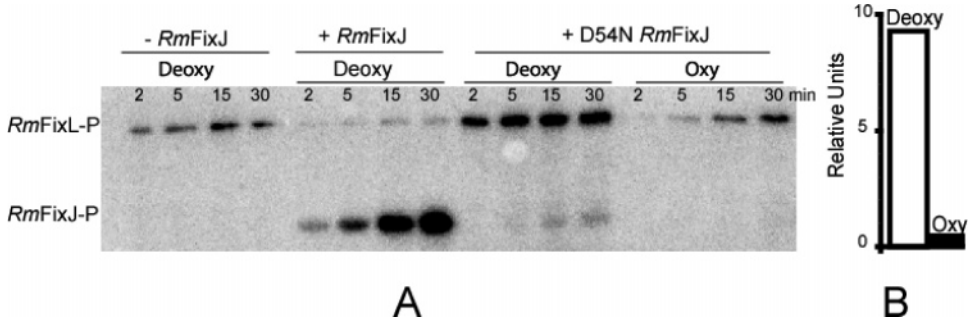

FIGURE 4: Effect of O_2 and D54N *Rm*FixJ on the phosphorylation of *Rm*FixL with ATP. Panel A shows an autoradiogram of the phosphorylation of *Rm*FixL (0.5 μM) with or without *Rm*FixJ (12.5 μM), or with D54N *Rm*FixJ (12.5 μM), under anaerobic and aerobic conditions, with 0.5 mM $MgCl_2$. The reactions were allowed to proceed for 2, 5, 15, and 30 min before quenching. Panel B compares the anaerobic and aerobic *Rm*FixL phosphorylations during the linear range of the reaction carried out with the *Rm*FixL−D54N *Rm*FixJ complex, as quantitated from the autoradiogram.

phoryl transfer to *Rm*FixJ occurs at the same rate, regardless of the introduction of O_2 (*15*). The experimental exclusion of the phosphoryl-transfer step further implies that O_2 probably does not regulate the dissociation of phospho-*Rm*FixJ from the phosphorylated complex. If this were the sole regulated step, turnover reactions in the presence of O_2 would generate phospho-*Rm*FixJ trapped in a complex, unable to dissociate, until all available *Rm*FixL reached the form of these dead-end, phosphorylated complexes.

The data given above clearly show that the initial reaction with ATP is the key ligand-regulated step in the transactions of the *Rm*FixL−*Rm*FixJ complex, although O_2 regulates neither binding of ATP nor complexation with *Rm*FixJ. *Rm*FixJ behaves as a potent allosteric enhancer of the phosphorylation of deoxy-*Rm*FixL.

DISCUSSION

In the phosphoryl transfers of the *Rm*FixLJ complex, O_2 regulates neither the affinity for ATP nor the complexation of the two proteins, but instead strongly inhibits an initial phosphorylation of *Rm*FixL (Figures 2−4). *Rm*FixJ accelerates the reaction with ATP, supplying a dramatic allosteric enhancement of this reaction under hypoxic conditions (Figure 4). The *Rm*FixL−*Rm*FixJ system is evolutionarily related to the large family of two-component regulatory systems that respond to a variety of signals (*10*). In addition, *Rm*FixL is functionally related to a broad class of heme-based sensor proteins that detect heme ligands (*41*).

Regulation of nucleotide binding, although ruled out for *Rm*FixLJ, may be a common feature of other sensors. For example, binding of NO causes a 30% to >80% drop in the K_m of the soluble guanylate cyclase (sGC) with respect to GTP, depending on the species (*42*, *43*); however, this step cannot entirely explain the more than 100-fold activation of sGC by NO. Complex formation would have been an interesting point for O_2 regulation of *Rm*FixLJ, but our results show that this is not the case. Work on the *E. coli* chemotaxis system has indicated that aspartate may regulate formation of the CheA−CheW−aspartate receptor ternary complex, suggesting that in some systems the signal may target complex formation for regulation (*44*).

Complex formation as a point for allosteric control plays a critical role in the phosphoryl transfers of the *Rm*FixL−*Rm*FixJ system and clearly demonstrates that *Rm*FixJ is an active partner in regulation, rather than merely a substrate of *Rm*FixL (*16*, *24*, *41*). The importance of complex formation is suggested by several other studies of two-component regulatory systems. For example, the *E. coli* CheW protein enhances the autokinase activity of CheA in the presence of the aspartate receptor (*40*). Interestingly, unlike *Rm*FixJ, which also functions as a substrate of *Rm*FixL, the CheW protein is not a substrate of CheA. So the chemotaxis system suggests a model in which the allosteric and final response regulations have been parceled to individual proteins. In another system that regulates sensing of dicarboxylic acids, formation of the DcuS−DcuR complex causes a modest enhancement (1.4-fold) of DcuS autophosphorylation (*45*). Although it is unlikely that allosteric behavior will be manifested in all two-component systems, our data, along with these reports, support the view that in many cases the reactions in a complex are more critical and physiologically relevant than those suggested by a sequential model.

The phosphorylation of *Rm*FixL proved to be the only one of the four examined steps regulated by O_2 in the *Rm*FixLJ complex. Moreover, we found that this was not accomplished by any effect of O_2 on the affinity of *Rm*FixL for nucleotide or *Rm*FixJ. The additional finding of a robust enhancement of the *Rm*FixL phosphorylation by *Rm*FixJ brings this reaction step into special focus and raises questions about the mechanisms by which protein−protein interactions and signal binding modify reactivity. Some possibilities include improved orientation of catalytical residues, alteration of their pK_a values, and minimization of structural fluctuations in the catalytical site. A detailed mechanistic analysis of the *Rm*FixL phosphorylation step of the *Rm*FixLJ complex is certain to expand our knowledge of O_2 sensing by this system and have interesting implications for related signal transducers.

ACKNOWLEDGMENT

We thank Ana C. S. Gondim for technical assistance, Jason R. Tuckerman for stimulating discussions, and Dr. Wen-Hong Li for generous access to his laboratory.

REFERENCES

1. David, M., Daveran, M. L., Batut, J., Dedieu, A., Domergue, O., Ghai, J., Hertig, C., Boistard, P., and Kahn, D. (1988) Cascade regulation of nif gene expression in *Rhizobium meliloti*, *Cell 54*, 671−683.
2. Soupene, E., Foussard, M., Boistard, P., Truchet, G., and Batut, J. (1995) Oxygen as a key developmental regulator of *Rhizobium*

meliloti N2-fixation gene expression within the alfalfa root nodule, *Proc. Natl. Acad. Sci. U.S.A. 92*, 3759−3763.
3. Anthamatten, D., and Hennecke, H. (1991) The regulatory status of the fixL- and fixJ-like genes in *Bradyrhizobium japonicum* may be different from that in *Rhizobium meliloti*, *Mol. Gen. Genet. 225*, 38−48.
4. Virts, E. L., Stanfield, S. W., Helinski, D. R., and Ditta, G. S. (1988) Common regulatory elements control symbiotic and microaerobic induction of nifA in *Rhizobium meliloti*, *Proc. Natl. Acad. Sci. U.S.A. 85*, 3062−3065.
5. Mesa, S., Bedmar, E. J., Chanfon, A., Hennecke, H., and Fischer, H. M. (2003) *Bradyrhizobium japonicum* NnrR, a denitrification regulator, expands the FixLJ-FixK2 regulatory cascade, *J. Bacteriol. 185*, 3978−3982.
6. Kaminski, P. A., and Elmerich, C. (1991) Involvement of fixLJ in the regulation of nitrogen fixation in *Azorhizobium caulinodans*, *Mol. Microbiol. 5*, 665−673.
7. Lopez, O., Morera, C., Miranda-Rios, J., Girard, L., Romero, D., and Soberon, M. (2001) Regulation of gene expression in response to oxygen in *Rhizobium meliloti*: Role of FnrN in fixNOQP expression and in symbiotic nitrogen fixation, *J. Bacteriol. 183*, 6999−7006.
8. Dixon, R., and Kahn, D. (2004) Genetic regulation of biological nitrogen fixation, *Nat. Rev. Microbiol. 2*, 621−631.
9. Aizawa, S. I., Harwood, C. S., and Kadner, R. J. (2000) Signaling components in bacterial locomotion and sensory reception, *J. Bacteriol. 182*, 1459−1471.
10. Stock, A. M., Robinson, V. L., and Goudreau, P. N. (2000) Two-component signal transduction, *Annu. Rev. Biochem. 69*, 183−215.
11. Foussard, M., Cabantous, S., Pedelacq, J., Guillet, V., Tranier, S., Mourey, L., Birck, C., and Samama, J. (2001) The molecular puzzle of two-component signaling cascades, *Microbes Infect. 3*, 417−424.
12. Hoch, J. A., and Varughese, K. I. (2001) Keeping signals straight in phosphorelay signal transduction, *J. Bacteriol. 183*, 4941−4949.
13. West, A. H., and Stock, A. M. (2001) Histidine kinases and response regulator proteins in two-component signaling systems, *Trends Biochem. Sci. 26*, 369−376.
14. Gilles-Gonzalez, M. A., Ditta, G. S., and Helinski, D. R. (1991) A haemoprotein with kinase activity encoded by the oxygen sensor of *Rhizobium meliloti*, *Nature 350*, 170−172.
15. Gilles-Gonzalez, M. A., and Gonzalez, G. (1993) Regulation of the kinase activity of heme protein FixL from the two-component system FixL/FixJ of *Rhizobium meliloti*, *J. Biol. Chem. 268*, 16293−16297.
16. Tuckerman, J. R., Gonzalez, G., Dioum, E. M., and Gilles-Gonzalez, M. A. (2002) Ligand and oxidation-state specific regulation of the heme-based oxygen sensor FixL from *Sinorhizobium meliloti*, *Biochemistry 41*, 6170−6177.
17. Reyrat, J. M., David, M., Blonski, C., Boistard, P., and Batut, J. (1993) Oxygen-regulated in vitro transcription of *Rhizobium meliloti* nifA and fixK genes, *J. Bacteriol. 175*, 6867−6872.
18. Agron, P. G., Ditta, G. S., and Helinski, D. R. (1993) Oxygen regulation of nifA transcription in vitro, *Proc. Natl. Acad. Sci. U.S.A. 90*, 3506−3510.
19. Gilles-Gonzalez, M. A., and Gonzalez, G. (2004) Signal transduction by heme-containing PAS-domain proteins, *J. Appl. Physiol. 96*, 774−783.
20. Dunham, C. M., Dioum, E. M., Tuckerman, J. R., Gonzalez, G., Scott, W. G., and Gilles-Gonzalez, M. A. (2003) A distal arginine in oxygen-sensing heme-PAS domains is essential to ligand binding, signal transduction, and structure, *Biochemistry 42*, 7701−7708.
21. Monson, E. K., Ditta, G. S., and Helinski, D. R. (1995) The oxygen sensor protein, FixL, of *Rhizobium meliloti*. Role of histidine residues in heme binding, phosphorylation, and signal transduction, *J. Biol. Chem. 270*, 5243−5250.
22. Reyrat, J. M., David, M., Batut, J., and Boistard, P. (1994) FixL of *Rhizobium meliloti* enhances the transcriptional activity of a mutant FixJD54N protein by phosphorylation of an alternate residue, *J. Bacteriol. 176*, 1969−1976.
23. Da Re, S., Schumacher, J., Rousseau, P., Fourment, J., Ebel, C., and Kahn, D. (1999) Phosphorylation-induced dimerization of the FixJ receiver domain, *Mol. Microbiol. 34*, 504−511.
24. Tuckerman, J. R., Gonzalez, G., and Gilles-Gonzalez, M. A. (2001) Complexation precedes phosphorylation for two-component regulatory system FixL/FixJ of *Sinorhizobium meliloti*, *J. Mol. Biol. 308*, 449−455.
25. Plesniak, L., Horiuchi, Y., Sem, D., Meinenger, D., Stiles, L., Shaffer, J., Jennings, P. A., and Adams, J. A. (2002) Probing the nucleotide binding domain of the osmoregulator EnvZ using fluorescent nucleotide derivatives, *Biochemistry 41*, 13876−13882.
26. Hiratsuka, T. (2003) Fluorescent and colored trinitrophenylated analogs of ATP and GTP, *Eur. J. Biochem. 270*, 3479−3485.
27. Stewart, R. C., VanBruggen, R., Ellefson, D. D., and Wolfe, A. J. (1998) TNP-ATP and TNP-ADP as probes of the nucleotide binding site of CheA, the histidine protein kinase in the chemotaxis signal transduction pathway of *Escherichia coli*, *Biochemistry 37*, 12269−12279.
28. Gilles-Gonzalez, M. A., Gonzalez, G., Perutz, M. F., Kiger, L., Marden, M. C., and Poyart, C. (1994) Heme-based sensors, exemplified by the kinase FixL, are a new class of heme protein with distinctive ligand binding and autoxidation, *Biochemistry 33*, 8067−8073.
29. Bradford, M. M. (1976) A rapid and sensitive method for the quantitation of microgram quantities of protein utilizing the principle of protein-dye binding, *Anal. Biochem. 72*, 248−254.
30. Hiratsuka, T., and Uchida, K. (1973) Preparation and properties of 2′(or 3′)-O-(2,4,6-trinitrophenyl) adenosine 5′-triphosphate, an analog of adenosine triphosphate, *Biochim. Biophys. Acta 320*, 635−647.
31. Head, C. G., Tardy, A., and Kenney, L. J. (1998) Relative binding affinities of OmpR and OmpR-phosphate at the ompF and ompC regulatory sites, *J. Mol. Biol. 281*, 857−870.
32. Laemmli, U. K. (1970) Cleavage of structural proteins during the assembly of the head of bacteriophage T4, *Nature 227*, 680−685.
33. Bilwes, A. M., Quezada, C. M., Croal, L. R., Crane, B. R., and Simon, M. I. (2001) Nucleotide binding by the histidine kinase CheA, *Nat. Struct. Biol. 8*, 353−360.
34. Birck, C., Malfois, M., Svergun, D., and Samama, J. (2002) Insights into signal transduction revealed by the low resolution structure of the FixJ response regulator, *J. Mol. Biol. 321*, 447−457.
35. Li, J., Swanson, R. V., Simon, M. I., and Weis, R. M. (1995) The response regulators CheB and CheY exhibit competitive binding to the kinase CheA, *Biochemistry 34*, 14626−14636.
36. Stewart, R. C., and VanBruggen, R. (2004) Phosphorylation and binding interactions of CheY studied by use of Badan-labeled protein, *Biochemistry 43*, 8766−8777.
37. Mattison, K., and Kenney, L. J. (2002) Phosphorylation alters the interaction of the response regulator OmpR with its sensor kinase EnvZ, *J. Biol. Chem. 277*, 11143−11148.
38. Cai, S. J., and Inouye, M. (2002) EnvZ-OmpR interaction and osmoregulation in *Escherichia coli*, *J. Biol. Chem. 277*, 24155−24161.
39. Stock, A., Koshland, D. E., Jr., and Stock, J. (1985) Homologies between the *Salmonella typhimurium* CheY protein and proteins involved in the regulation of chemotaxis, membrane protein synthesis, and sporulation, *Proc. Natl. Acad. Sci. U.S.A. 82*, 7989−7993.
40. Ninfa, E. G., Stock, A., Mowbray, S., and Stock, J. (1991) Reconstitution of the bacterial chemotaxis signal transduction system from purified components, *J. Biol. Chem. 266*, 9764−9770.
41. Gilles-Gonzalez, M. A., and Gonzalez, G. (2005) Heme-based sensors: Defining characteristics, recent developments, and regulatory hypotheses, *J. Inorg. Biochem. 99*, 1−22.
42. Chang, F. J., Lemme, S., Sun, Q., Sunahara, R. K., and Beuve, A. (2005) Nitric oxide-dependent allosteric inhibitory role of a second nucleotide binding site in soluble guanylyl cyclase, *J. Biol. Chem. 280*, 11513−11519.
43. Ruiz-Stewart, I., Tiyyagura, S. R., Lin, J. E., Kazerounian, S., Pitari, G. M., Schulz, S., Martin, E., Murad, F., and Waldman, S. A. (2004) Guanylyl cyclase is an ATP sensor coupling nitric oxide signaling to cell metabolism, *Proc. Natl. Acad. Sci. U.S.A. 101*, 37−42.
44. Homma, M., Shiomi, D., Homma, M., and Kawagishi, I. (2004) Attractant binding alters arrangement of chemoreceptor dimers within its cluster at a cell pole, *Proc. Natl. Acad. Sci. U.S.A. 101*, 3462−3467.
45. Janausch, I. G., Garcia-Moreno, I., Lehnen, D., Zeuner, Y., and Unden, G. (2004) Phosphorylation and DNA binding of the regulator DcuR of the fumarate-responsive two-component system DcuSR of *Escherichia coli*, *Microbiology 150*, 877−883.

BI051661H